

## Rheological instability in a simple shear thickening model

D. A. HEAD<sup>1</sup>, A. AJDARI<sup>2</sup> and M. E. CATES<sup>1</sup>

<sup>1</sup> *Department of Physics and Astronomy, JCMB King's Buildings, University of Edinburgh, Edinburgh EH9 3JZ, UK*

<sup>2</sup> *Laboratoire de Physico-Chimie Théorique, Esa CNRS 7083, ESPCI, 10 rue Vauquelin, F-75231 Paris Cedex 05, France*

PACS. 83.60.Rs – Shear rate-dependent structure (shear thinning and shear thickening).

PACS. 83.60.Wc – Flow instabilities.

PACS. 82.40.Bj – Oscillations, chaos, and bifurcations.

**Abstract.** – We study the strain response to steady imposed stress in a spatially homogeneous, scalar model for shear thickening, in which the local rate of yielding  $\Gamma(l)$  of mesoscopic ‘elastic elements’ is not monotonic in the local strain  $l$ . Despite this, the macroscopic, steady-state flow curve (stress vs. strain rate) is monotonic. However, for a broad class of  $\Gamma(l)$ , the response to steady stress is not in fact steady flow, but spontaneous oscillation. We discuss this finding in relation to other theoretical and experimental flow instabilities. Within the parameter ranges we studied, the model does not exhibit rheo-chaos.

The flow behaviour of shear-thickening materials such as dense colloidal suspensions can be complex [1,2]. For example, imposition of a steady mean strain rate can lead to large, possibly chaotic, variations in the mean stress [1]. The same occurs in some types of shear-thickening micellar surfactant solutions, where true temporal chaos seems now to be established [3]. Other unexpected behaviour, such as a bifurcation to an oscillatory state, has also been seen in shear-thickening ‘onion’ phases of surfactant [4]. It is not yet known to what extent such unsteady flow is generic in shear-thickening systems; in this letter we attempt to shed some light on the issue by studying a much-simplified, generic model. In this model we find, for a wide range of parameters, spontaneous rheological oscillation of the strain rate at fixed stress. Rheo-chaos is, however, not found for the parameters studied so far.

A feature that distinguishes the rheological instabilities encountered in shear-thickening from those arising in Newtonian fluids is that the nonlinearity is not inertial (not from the advective term of the Navier Stokes equation): the Reynolds number is essentially zero [5]. Instead it arises from anharmonic elastic responses at large deformations, complicated and perhaps strongly enhanced by the presence of memory effects. Flow instabilities leading to chaos have been studied recently by Grosso *et al.* [6] in a model for suspended rodlike particles. As that work shows, and our work confirms, temporal instabilities can arise even in a model where macroscopic spatial inhomogeneity is disallowed altogether. This is a strong demarcation from the familiar shear-banding instabilities that arise whenever the steady-state flow curve is nonmonotonic (the flow curve is the function  $\sigma(\dot{\gamma})$ , where  $\sigma$  is shear stress and  $\dot{\gamma}$  the rate of shear strain) [7,8]. Shear banding is well documented in shear thinning materials

(particularly micelles [8]) but also possible in shear thickening ones [9], albeit with a different spatial organization of the bands of coexisting material. However it is not the subject of this Letter – we are interested in *temporal* inhomogeneity.

Our simplified model of a shear thickening fluid is defined as follows. We imagine an ensemble of mesoscopic elastic elements, each having a local strain variable  $l$ . We consider only simple shear strains, and neglect normal stresses, so that the only nontrivial stress is the corresponding shear stress  $\sigma$ . (These assumptions reduce the problem to a scalar one.) Let us define  $P(l, t)$  to be the probability density function of elements which have a local strain  $l$  at time  $t$ . We assume  $P(l, t)$  evolves in time according to two distinct mechanisms: homogeneous shearing at a rate  $\dot{\gamma}$ , and the yielding of elements at a rate  $\Gamma(l)$  per unit time. In calculating the stress, the elements are supposed to behave elastically between yield events, so that the local stress is just  $kl$ , where  $k > 0$  is an elastic constant. The global stress  $\sigma$  is simply the arithmetic mean of the local stresses, or  $\sigma = \langle kl \rangle = k \langle l \rangle$ . (Here the angled brackets represent an instantaneous average over  $P(l, t)$ .) We ignore completely the fact that, in practice, the strain rate  $\dot{\gamma}$  can vary locally in space in response to each mesoscopic element having a different local stress.

In the present work,  $\Gamma(l)$  is the same for all elements, which simplifies the analysis significantly. A more comprehensive model, in which elements each have their own ‘yield strain’  $E$  is studied in a longer paper [10], where further details of some of our calculations can also be found. Both models are closely related to the (shear-thinning) SGR model of Sollich *et al.* [11], but we will choose a very different form of  $\Gamma(l)$  from that of SGR.

The master equation for  $P(l, t)$  is then

$$\frac{\partial P}{\partial t} + \dot{\gamma} \frac{\partial P}{\partial l} = -\Gamma(l)P + \omega(t) \delta(l) \quad (1)$$

The second term on the left-hand side represents the increase in local strains  $l$  according to the spatially uniform strain rate  $\dot{\gamma}$ . The two terms on the right hand side describe the birth and death of elements with strain  $l$ , respectively, where  $\delta(l)$  reflects the assumption that newly-yielded elements are unstrained. The total rate of yielding  $\omega(t)$  is defined by

$$\omega(t) = \int_{-\infty}^{\infty} dl \Gamma(l)P(l, t) = \langle \Gamma(l) \rangle \quad (2)$$

The key remaining ingredient of our model is the hopping rate  $\Gamma(l)$ . We parameterise this as follows:

$$\Gamma(l) = \Gamma_0 \exp \left[ - \left( E - kl^2/2 \right) / x(l) \right] \quad (3)$$

This is a pseudo-activated form, in which each element is subject to an effective temperature  $x$ , and attempts (at a rate  $\Gamma_0$ ) to hop over a barrier of height  $E - \frac{1}{2}kl^2$ . The latter expression allows for the lowering of the elastic yield barrier by the imposition of strain; on its own this will always lead to shear thinning.

However, the novel feature in the current model is to allow  $x(l)$  to be a decreasing function of  $l$ . This reflects the intuition that, even if a small local stress or strain always promotes yield, a large enough one may jam an element against its neighbours causing the jump rate to fall. Other than in steady state (see below) we have been unable to find an analytic solution to (1) for any non-trivial  $x(l)$ . Instead it has been numerically integrated. With the above as motivation, we chose for numerical purposes relatively simple (piecewise constant) decreasing functions  $x(l)$ . The precise choice of  $x(l)$  — in particular, whether it is smooth or not — does not seem to qualitatively influence the results.

*Results.* – The steady state solution  $P_\infty(l)$  of (1) is found as (setting  $k = \Gamma_0 = 1$  from now on, for convenience)

$$P_\infty(l) = \omega_\infty \dot{\gamma}^{-1} \exp[-\dot{\gamma}^{-1} f(l)] \quad (4)$$

where  $f(l) \equiv \int_0^l dl' \Gamma(l')$ , and  $\omega_\infty$ , the asymptotic jump rate, is fixed by normalization of  $P_\infty$ . It is straightforward to show from (4) that in the limit of slow flows  $\dot{\gamma} \rightarrow 0^+$ , the steady state stress response  $\sigma_\infty = \langle l \rangle_\infty$  (in an obvious notation) is always linear:  $\sigma_\infty \sim \dot{\gamma} e^{E/x(0)}$ . Hence there is no yield stress for any choice of  $x(0)$ . This contrasts with a model having an exponential distribution of barrier heights  $E$  for different elements, which does show onset of a yield stress, connected with the presence of a glass transition, as  $x$  is reduced [11]. For monodisperse  $E$ , as here, there is no such transition.

We now show that the steady state flow curve, for *any* choice of function  $x(l)$ , has a monotonically increasing  $\sigma(\dot{\gamma})$ . First, by differentiating  $\langle l \rangle_\infty$  and using (4), we find

$$\frac{\partial \sigma_\infty}{\partial \dot{\gamma}} = \frac{\sigma_\infty}{\omega_\infty} \frac{\partial \omega_\infty}{\partial \dot{\gamma}} - \frac{\sigma_\infty}{\dot{\gamma}} + \frac{1}{\dot{\gamma}^2} \langle lf \rangle_\infty \quad (5)$$

Similarly, the normalisation integral for  $P_\infty$  can be differentiated with respect to  $\dot{\gamma}$  to give

$$\frac{1}{\omega_\infty} \frac{\partial \omega_\infty}{\partial \dot{\gamma}} = \frac{1}{\dot{\gamma}} - \frac{1}{\dot{\gamma}^2} \langle f \rangle_\infty \quad (6)$$

Combining these two expressions (with  $\sigma_\infty = \langle l \rangle_\infty$ ) produces

$$\dot{\gamma}^2 \frac{\partial \sigma_\infty}{\partial \dot{\gamma}} = \langle lf \rangle_\infty - \langle l \rangle_\infty \langle f \rangle_\infty \quad (7)$$

which is positive since  $f(l)$  is monotone increasing. Thus there are no regions on the flow curve with negative slope, and for no choice of  $x(l)$  does one expect any shear-banding instability to arise. However, the argument does not prove that a steady state is ever actually achieved. We have found that it is reached under conditions of imposed strain  $\gamma(t)$ , but *not* under an imposed stress  $\sigma$  (for appropriate  $x(l)$ ), for which the model exhibits temporal oscillations instead.

This numerical finding (detailed below) is also supported by a linear stability analysis for perturbations about the steady state flow, described fully in [10]. Such an analysis shows that the transient behaviour close to steady state is never a real exponential decay but always has an oscillatory component. When the decay rate of these oscillations changes sign, the flow becomes unstable to permanent oscillation.

*The oscillatory regime.* – The time evolution of the system at fixed stress was studied numerically by methods described in [10]. (The problem is not standard and significant amounts of computer time were required to achieve reliable results.) A range of different functions  $x(l)$  and of  $E$  values were tried. Varying  $\sigma$  over a wide range of values in each case reveals that steady flow is always reached for sufficiently small and sufficiently large imposed stresses; but for intermediate  $\sigma$ , an oscillatory regime is observed whenever  $x(l)$  is strongly enough decreasing. It is impractical to explore the entire function space for  $x(l)$  so at present the precise criteria for the presence of oscillations are not known.

Within the oscillatory regime, we have so far found only single-period oscillations with no sign of period doubling or other more complex nonsteady behaviour that might point to the onset of rheo-chaos in some parts of the parameter space. Some examples of the oscillatory

behaviour are given in Fig. 1(a). To obtain these results we took  $x = 1$  for  $l < 0.4$  and  $x = 0.4$  for  $l > 0.4$ ; in addition we set  $E = 5$ . The strain  $\gamma(t)$  is shown for three different imposed  $\sigma$ . On close inspection the oscillations, after a brief transient, appear perfectly periodic. This applies not only in the stress but in the underlying distribution  $P(l, t)$ , which determines the future evolution. Hence there seems little doubt that these oscillations will persist indefinitely.

From Fig. 1(a) it is remarkable that the *mean* strain rate  $\bar{\dot{\gamma}}$ , defined as  $\dot{\gamma}$  averaged over a single period of oscillation, is clearly a *decreasing* function of  $\sigma$ , in complete contrast to the monotonic, steady state, flow curve. The time averaged values  $\bar{\dot{\gamma}}$  as read off from the simulations are plotted against  $\sigma$  in Fig. 1(b), overlaid with the steady state flow curve. Within the oscillatory regime, the  $\bar{\dot{\gamma}}$  line deviates from the flow curve to the extent that it loses monotonicity over a large interval of  $\sigma$ . If the oscillations were not detected but only the average behaviour measured, this would resemble the flow curve of a discontinuously shear-thickening system close to a jamming transition, although in that case shear banding could be expected as well. (Such a flow curve is indeed found in models where  $x$  depends not on the local stress  $l$  but only on its global mean,  $\sigma$ ; see [10].)

Upper and lower transition points between oscillatory and steady flow can be seen in the figure. At each transition point  $\sigma = \sigma_c$ , the period of oscillation remains finite whilst the amplitude vanishes smoothly according to  $|\sigma - \sigma_c|^\alpha$  with  $\alpha > 0$ . As we discuss in our longer work [10], technical difficulties have prevented us from reliably fixing the asymptotic values of  $\alpha$ . In particular we have been unable to rule out  $\alpha = 0.5$  for both transitions, as expected for a Hopf bifurcation [4, 12] (although since the control parameter is an integral constraint, it is not clear to us if it should be a Hopf bifurcation).

Though always perfectly periodic, the waveform of the oscillations varies with  $\sigma$ . Close to either transition, the oscillations are near-sinusoidal, as demonstrated in Fig. 2(a). Further into the oscillatory regime,  $\dot{\gamma}$  can no longer be decomposed into a single harmonic, but instead approaches a waveform in which most of the variation in  $\dot{\gamma}$  is compressed into a small fraction of the total period of oscillation. An example is given in Fig. 2(b). This behaviour at first appears to be similar to the ‘stick–slip’ motion observed in systems such as earthquakes [14], ultra-thin liquid films [15] and granular media [16, 17]. However, the underlying physics in our model seems to be somewhat different to these examples. Indeed, stick–slip is usually viewed as a surface phenomenon, whereas the model studied in this paper has no surface and describes only bulk effects. Irrespective of the waveform, the product of  $\bar{\dot{\gamma}}$  and the period of oscillation  $T$  is approximately constant,  $l^* = \bar{\dot{\gamma}}T \approx 2.3$  for this example. This will be explained below in terms of the evolution of  $P(l, t)$ .

*Mechanism of oscillation.* – Snapshots of  $P(l, t)$  during a single period of oscillation are given in Fig. 3. The mechanism behind the oscillations can be qualitatively described in terms of two coexisting populations of elements — a ‘hot’ population of unstrained or slightly strained elements with  $l \approx 0$ , and hence a high effective temperature  $x(l)$ ; and a ‘cold’ population of elements with  $l \gg 0$  and therefore a low  $x(l)$ . Starting at a time when  $\dot{\gamma}(t)$  is near to its minimum value, corresponding to the first snapshot in the figure, the stress-weighted yield rate  $\langle l\Gamma(l) \rangle$  for both populations of elements is low. This is because the hot elements have small  $l$ , whereas the cold elements have a low yield rate  $\Gamma(l)$ . Thus the strain rate  $\dot{\gamma}$  required to maintain the imposed constant mean stress  $\sigma$ , which is  $\dot{\gamma}(t) = \langle l\Gamma(l) \rangle$  (as seen by multiplying (1) by  $l dl$  and integrating), is also low.

Although  $\dot{\gamma}(t)$  is small in this state, it is nonetheless non-zero, and therefore the strains  $l$  of the cold elements increase according to  $\dot{l} = \dot{\gamma}$ . This decreases their effective energy barrier  $E - l^2/2$ , increasing their hop rate and therefore the rate of stress lost due to cold elements yielding. Thus  $\dot{\gamma}(t) = \langle lP(l) \rangle$  will also increase, which accelerates the rate at which the cold

elements yield, and so on. This description is that of a *positive feedback loop* that causes  $\dot{\gamma}$  to increase at ever faster rates until all of the cold elements have been depleted. The second snapshot in Fig. 3 show the state of the system shortly before this has happened.

While  $\dot{\gamma}(t)$  is high, the hot elements are becoming rapidly strained and have little time to yield before crossing over into the cold region with large  $l$ . Thus  $P(l, t)$  is flat for small  $l$ . As  $\dot{\gamma}(t)$  again decreases, this flat part of the distribution will start to decay as the elements within it yield. However, the yield rate depends on  $x(l)$ , and since this changes to a lower value at  $l = 0.4$ ,  $P(l, t)$  will decay more rapidly for  $l$  smaller than 0.4 than for  $l$  greater than 0.4. Thus a dip will occur around the point  $l \approx 0.4$ , which can clearly be seen in Fig. 3. This dip becomes more pronounced with time until the system can again be viewed as coexisting ‘hot’ and ‘cold’ populations, when the cycle begins again.

A possible interpretation of the parameter  $l^*$ , defined previously, is that it is the amount by which the system needs to be strained until the positive feedback loop just described starts to dominate the system behaviour, causing it to ‘reset’ to the start of its cycle. If this is correct, then  $l^*$  should correspond to the point at which highly-strained elements have the same yield rate as unstrained elements, *i.e.*  $\Gamma(0) \approx \Gamma(l^*)$ . Rough calculations based on this assumption give  $l^* \approx \sqrt{2E[1 - x(\infty)/x(0)]}$ , which for this example predicts  $l^* \approx 2.4$ , in fair agreement with the observed value.

*Discussion.* – Within a simple model of shear thickening, we have found regimes where steady flow at constant imposed stress is unstable and temporal oscillation occurs instead. Known instances of such rheological instability have often been explained in terms of the spatial coexistence of subpopulations, or phases. For instance, the temporal oscillations in viscosity observed in wormlike micelles under an imposed stress was attributed to a slowly fluctuating interface between a fluid phase and shear-induced structures [13]. For surfactant solutions in the lyotropic lamellar phase, it was attributed to coexisting ordered and disordered phases [4]. By contrast, the temporal oscillations observed in our model arise even though they are by assumption spatially homogeneous, and the flow curves are everywhere monotonic. It may be that, in practice, such rheo-oscillations will always be coupled to spatial heterogeneity of some sort. Experiments are not advanced enough to indicate whether this is the case.

One distinguishing feature of our equations is the role of memory effects, rather than inertia, in allowing oscillations. In our model, the memory resides in  $P(l, t)$  which can have different shapes for the same applied stress  $\langle l \rangle$ . There may thus be a link to work on ‘delay differential equations’ in which a first order differential equation for a state variable contains a feedback term that depends on the same state variable at an earlier time [18]. Such equations are capable of showing a range of instabilities, including chaos, despite the absence of inertia. The nature of this link remains a topic of current research. Its exploration might help answer the following question: what features, if any, could be added to our simple rheological model of shear thickening to allow rheo-chaos to arise *without* coupling to spatial degrees of freedom [6]. This could in turn help answer another important question: what is the dimension of the strange attractors that arise in rheo-chaos [3]? In conclusion we suggest that the study of temporal (or spatiotemporal) pattern formation in non-Newtonian flows (at effectively zero Reynolds number) will form a major topic of experimental and theoretical research in the coming years.

## REFERENCES

- [1] LAUN H.M., *J. Non-Newton. Fluid Mech.*, **54** (1994) 87.

- [2] MELROSE J.R. and BALL R.C., *Europhys. Lett.*, **32** (1995) 535; CATHERALL A.A., MELROSE J.R. and BALL R.C., *J. Rheol.*, **44** (2000) 1.
- [3] BANDYOPADHYAY R., BASAPPA G. and SOOD A.K., *Phys. Rev. Lett.*, **84** (2000) 2022.
- [4] WUNENBURGER A.S, COLIN A., LENG J., ARNÉDO A. and ROUX D., *Phys. Rev. Lett.*, **86** (2001) 1374.
- [5] GROISMAN A. and STEINBERG V., *Europhys. Lett.*, **43** (1998) 165.
- [6] GROSSO M., KEUNINGS R., CRESCITELLI S. and MAFFETTONE P.L, *Phys. Rev. Lett.*, **86** (2001) 3184.
- [7] MCLEISH T.C.B. and BALL R.C., *J. Poly. Sci. B*, **24** (1986) 1735.
- [8] SPENLEY N.A., CATES M.E. and MCLEISH T.C.B., *Phys. Rev. Lett.*, **71** (1993) 939.
- [9] OLMSTED P.D. and LU C.Y.D., *Faraday Disc.*, **112** (1999) 183.
- [10] HEAD D.A., AJDARI A. and CATES M.E., “*Jamming and oscillatory strain response in scalar models for shear thickening*”, Preprint, 2001.
- [11] SOLLICH P, LEQUEUX F., HÉBRAUD P. and CATES M.E., *Phys. Rev. Lett.*, **78** (1997) 2020.
- [12] GLENDINNING P., *Stability, instability, and chaos: an introduction to the theory of nonlinear differential equations* (Cambridge University Press, Cambridge) 1994.
- [13] HU Y.T., BOLTENHAGEN P. and PINE D.J., *J. Rheol.*, **42** (1998) 1185.
- [14] SCHOLZ C.H., *Nature*, **391** (1998) 37.
- [15] ARANSON I.S., TSIMRING L.S. and VINOKUR V.M., cond-mat/0101186 Preprint, 2001.
- [16] LUBERT M. and DE RYCK A., *Phys. Rev. E*, **63** (2001) 021502.
- [17] ALBERT I., TEGZES P., ALBERT R., SAMPLE J.G., BARABÁSI A.-L., VICSEK T. and SCHIFFER P., cond-mat/0102523 Preprint, 2001.
- [18] GLASS L and MACKEY M.C., *From Clocks to Chaos* (Princeton University Press, Princeton) 1988.

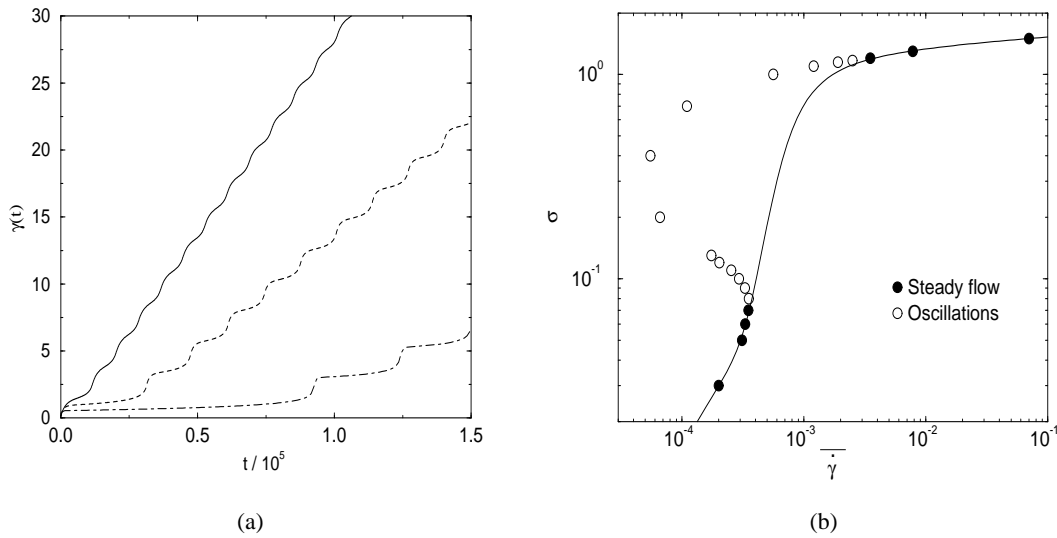


Fig. 1 – (a) The strain  $\gamma(t)$  under an imposed stress  $\sigma = 0.1$  (solid line), 0.13 (dashed line) and 0.2 (dot-dashed line) for  $x(l) = 1$  for  $l < 0.4$  and  $x = 0.4$  for  $l > 0.4$ . The system was initially unstrained and  $E = 5$ . (b) The mean strain rate  $\bar{\dot{\gamma}}$  against the imposed stress  $\sigma$  for the same system. The solid and filled circles represent steady and oscillatory solutions, respectively, as observed from the simulations. The sizes of the circles are larger than the error bars. For comparison, the theoretical flow curve for the steady state solution (4) is plotted as a solid line.

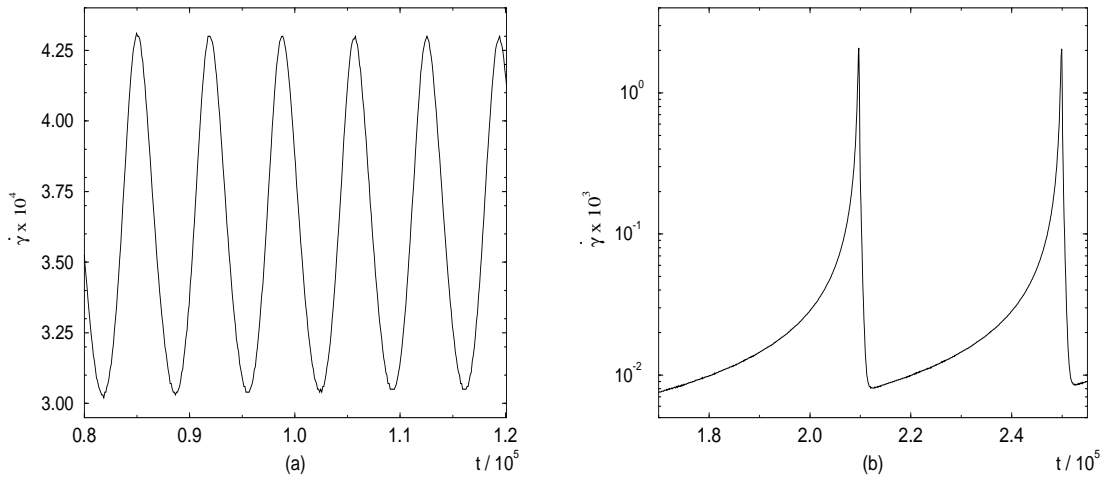


Fig. 2 – Examples of the oscillatory strain response to a constant stress for the same  $x(l)$  as in Fig. 1. The imposed stresses are (a)  $\sigma = 0.075$ , which is just above the threshold value for steady flow, and (b)  $\sigma = 0.4$ , which is well into the oscillatory regime. Note that the axes in (b) are semilogarithmic.

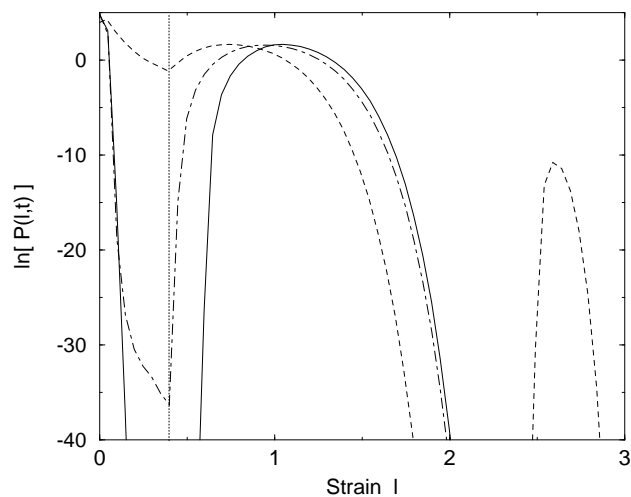


Fig. 3 – Snapshots of  $P(l, t)$  in a monodisperse system with  $E_1 = 5$ , and  $x(l) = 1$  for  $l < 0.4$ , 0.4 otherwise. The imposed stress was  $\sigma = 0.2$ . The times of each plot are  $t = 1.1 \times 10^5$  (solid line),  $t = 1.25 \times 10^5$  (dashed line) and  $t = 1.3 \times 10^5$  (dot-dashed line), corresponding to before, during and just after the peak in  $\dot{\gamma}$ , respectively. The vertical dotted line is where  $x(l)$  changes value. Note that this corresponds to the lower line in Fig. 1.